Mechanism for the Destabilization of the Dimer Interface in a Mutant HIV-1 Protease: A Molecular Dynamics Study

William E. Harte, Jr.,*,† and David L. Beveridge†

Contribution from the Chemistry Department, Hall-Atwater Laboratories, Wesleyan University, Middletown, Connecticut 06457, and Bristol-Myers Squibb Pharmaceutical Research Institute, 5 Research Parkway, Wallingford, Connecticut 06492. *Received June 26, 1992*

Abstract: A molecular dynamics simulation has been performed on the Asn88–Gln88 mutant of the aspartyl protease of the human immunodeficiency virus including explicit consideration of solvent water molecules. Studies of residue 88 protease mutants by Guenet et al. (*Eur. J. Pharmacol.* **1989**, *172*, 443–451) have previously demonstrated that the enzyme is inactivated due to dimer dissociation, even though the mutant site is removed from the dimer interface. The calculations provide leading evidence that the dimer is destabilized in the Gln88 mutant and suggest a molecular mechanism in which the mutation indirectly alters the articulation of the monomeric units.

Introduction

HIV-1 protease (HIV-1 PR) is an essential enzyme involved in the maturation of the human immunodeficiency virus.[1] HIV-1 PR, an aspartyl protease, hydrolyses the initial translation products of the gag and pol genes into functional proteins. This enzyme is the only macromolecular constituent of the AIDS virus for which a complete structure determination has been achieved by X-ray crystallography.[2-4] The active form of HIV-1 PR is a dimer, with the 99-residue monomeric units interacting via a dovetailed, β-pleated sheet involving both the C-terminal and N-terminal units of the polypeptide chain. The catalytic triads are located at residues 25–27 in each monomer.

HIV-1 protease has recently been studied in considerable detail via site-directed mutagenesis, and a number of sites which alter the enzymatic activity have been identified.[5,6] Most of these involve residues at or near the active site, but some occur in regions not directly implicated in the reaction mechanism. A series of mutants at Asn88 have led to significant alterations in the enzymatic activity.[5] Western blot analysis detected monomeric protease, indicating that the mutation caused dissociation of the protease dimer. The Gln88 mutant was reported to have no activity compared with the native. Since only the addition of a methylene group at some distance from the dimer interface is involved, this result was somewhat surprising. The position of residue 88 in the structure is shown in Figure 1.

Recently, we reported a series of molecular dynamics simulations on the HIV-1 protease dimer, treating both in vacuo and solvated models.[7-9] The simulation produced an accurate account of the crystal structure results only with the explicit inclusion of solvent waters.[9] Analysis of the atomic fluctuations revealed interesting dynamical correlations within the molecule and provided a possible explanation of the effect of mutations within the cantilever domain of the structure.[7] We describe herein a new MD simulation carried out on the Gln88 mutant of HIV-1 PR and consider on this basis the molecular nature of the effect of the mutation of the stability of the protease dimer.

Calculations

The MD in this study was performed with the Monte Carlo (MC) and MD simulation program WESDYN,[10] using the GROMOS86 force field[11] and the SPC model for water.[12] Switching functions were used to make the long-range nonbonded interactions go smoothly to 0 between 7.5 and 8.5 Å and were applied on a group-by-group basis to avoid artificially splitting dipoles. The initial structure for the protease in the simulation was the X-ray crystal form of HIV-1 PR solved by Wlodawer et al.[3] (deposited in the Brookhaven Data Bank as 3HVP,[13] modified by the addition of a methylene-united atom at Asn88, mutating it into a Gln residue. The side-chain torsional angles of Gln were adjusted to alleviate any steric crowding. The mutant protein was placed in a hexagonal prism of height 78.928 Å and inscribed radius of 34.562 Å and solvated with 6990 molecules of water. The volume was chosen to produce a solvent density of 1 g/cm^3. The central cell was treated under periodic boundary conditions in order to emulate a condensed-phase environment.

The simulation protocol included an initial solvent relaxation of 3K passes of Metropolis MC (21M configurations), followed by 50 steps of conjugate gradient minimization on the total system. The MD steps involved a heating to 300 K over 1.5 ps, a Gaussian equilibration step of 2.5 ps, and a trajectory involving 96 ps of free MD with a temperature window of 5 K. No rescaling was required beyond 25 ps into the run. Analysis was based on the interval between 30 and 100 ps in the simulation.

Results and Discussion

The convergence characteristics of the simulation together with the corresponding results obtained previously for the native protease are shown as a function of time in Figure 2. The total energy and temperature (Figure 2a,b) were observed to be stable after 25 ps. The root mean square (rms) deviation of the MD structures from the starting configuration as a function of time is a measure

* Address correspondence to this author at Bristol-Myers Squibb Pharmaceutical Research Institute.
† Wesleyan University.

(1) Kohl, N.; Emini, E. A.; Schlief, W. A.; Davis, L. J.; Heimbach, J.; Dixon, R. A. F.; Scolnik, E. M.; Sigal, I. S. *Proc. Natl. Acad. Sci. USA* **1988**, *85*, 4686–4690.
(2) Navia, M. A.; Fitzgerald, P. M. D.; McKeever, B. M.; Leu, C.; Heimbach, J. C.; Herber, W. K.; Segal, I. S.; Darke, P. L.; Springer, J. P. *Nature* **1989**, *337*, 615–620.
(3) Wlodawer, A.; Miller, M.; Jaskolski, M.; Sathyanarayana, B. K.; Baldwin, E.; Weber, J. T.; Selk, L. M.; Clawson, L.; Schneider, J.; Kent, S. B. H. *Science* **1989**, *245*, 616–621.
(4) Lipatto, R.; Blundell, T.; Hemmings, A.; Overington, J.; Wilderspin, A.; Wood, S.; Merson, J. R.; Whittle, P. J.; Danley, D. E.; Geogharan, K. F.; Hawrylik, S. J.; Lee, S. E.; Scheld, K. G.; Hobart, P. M. *Nature (London)* **1989**, *342*, 299–301.
(5) Guenet, C.; Leppik, R. A.; Pelton, J. T.; Moelling, K.; Lovenberg, W.; Harris, B. A. *Eur. J. Pharmacol.* **1989**, *172*, 443–451.
(6) Loeb, D. D.; Swanstrom, R.; Everitt, L.; Manchester, M.; Stamper, S. E.; Hutchinson, C. A., III *Nature* **1989**, *340*, 397–400.
(7) Harte, W. E., Jr.; Swaminathan, S.; Mansuri, M. M.; Martin, J. C.; Rosenberg, I. E.; Beveridge, D. L. *Proc. Natl. Acad. Sci. USA* **1990**, *87*, 8864–8868.
(8) Swaminathan, S.; Harte, W. E., Jr.; Beveridge, D. L. *J. Am. Chem. Soc.* **1991**, *113*, 2717–2721.
(9) Harte, W. E., Jr.; Swaminathan, S.; Beveridge, D. L. *Proteins: Struct., Funct., Genet.* **1992**, *13*, 175–194.
(10) Swaminathan, S. *WESDYN: Monte Carlo and Molecular Dynamics Computer Simulation of Macromolecules at Wesleyan*; Wesleyan University, Middletown, CT, 1990.
(11) van Gunsteren, W. F.; Berendsen, H. J. C. *GROMOS86: Groningen Molecular Simulation System*; University of Groningen, The Netherlands, 1986.
(12) Berendsen, H. J. C.; Postma, J. P. M.; van Gunsteren, W. F.; Hermans, J. In *Intermolecular Forces*; Pullman, B., Ed. D. Reidel: Dordrecht, 1981; pp 331–342.
(13) Bernstein, F. C.; Koetzel, T. G.; Williams, G. J. B.; Meyer, E. F., Jr.; Brice, M. D.; Rogers, J. R.; Kennard, O.; Shimanouchi, T.; Tasumi, M. *J. Mol. Biol.* **1977**, *112*, 535.

0002-7863/93/1515-1231$04.00/0

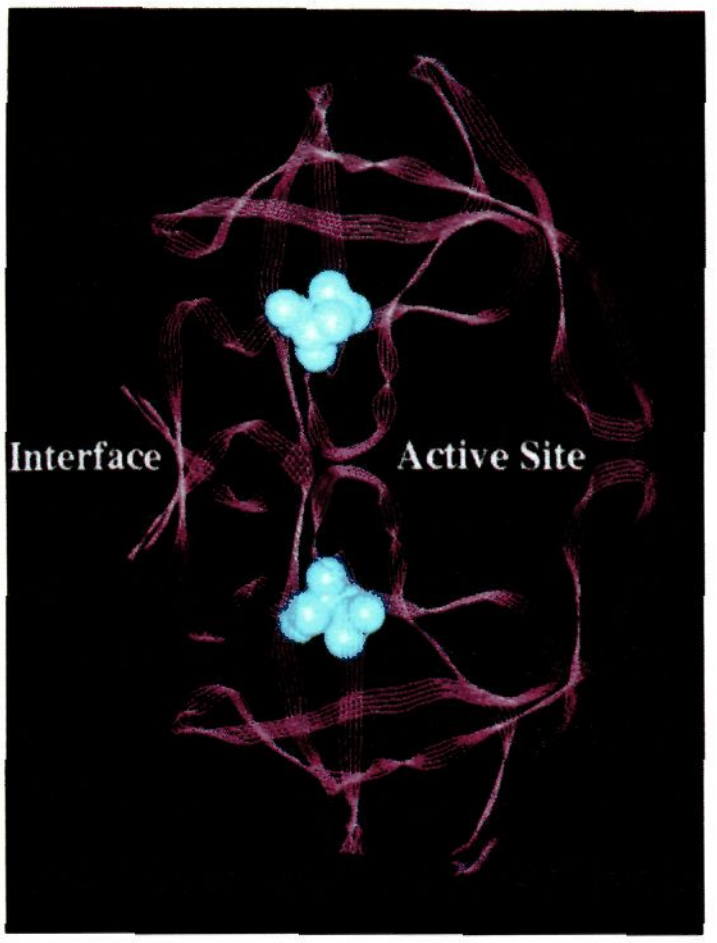

Figure 1. Ribbon trace of HIV-1 protease with CPK highlight of residue 88.

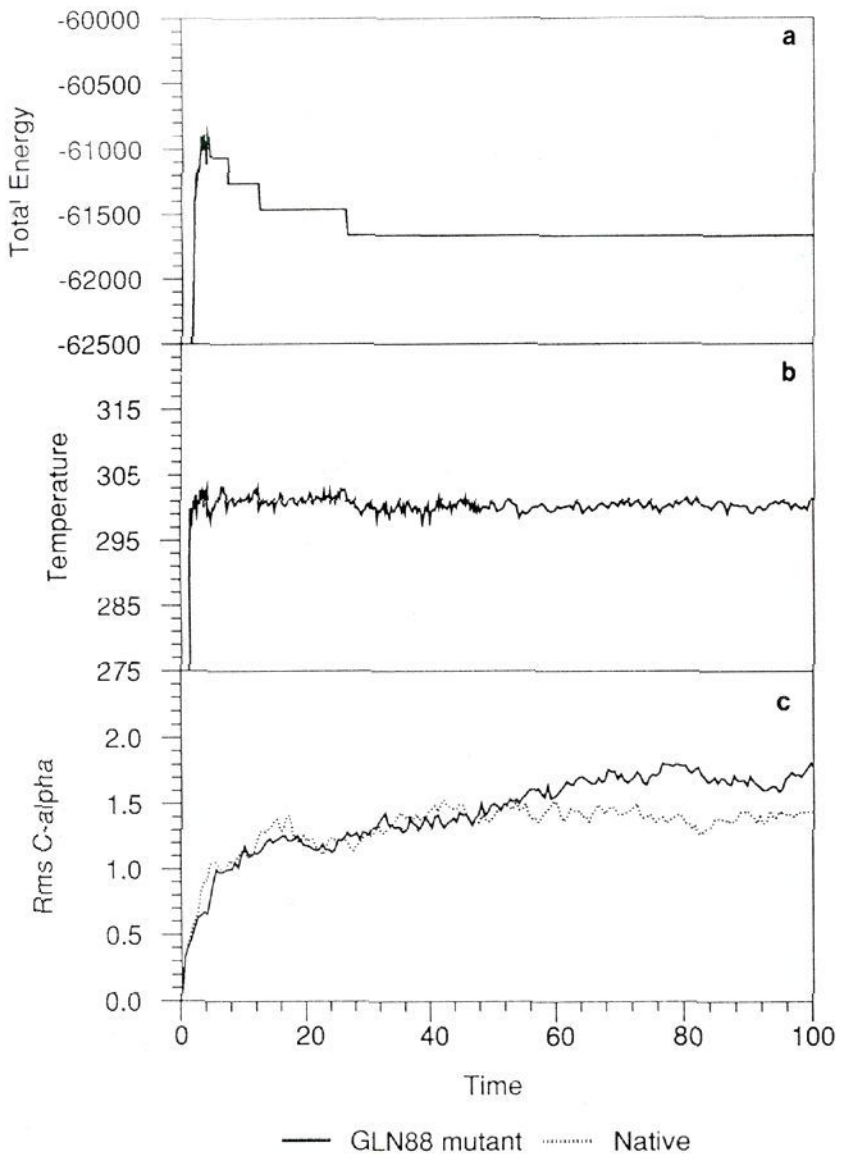

Figure 2. Calculated total energy, temperature, and root mean square deviation of dynamical structures from the 3HVP crystal geometry (**3**) vs time from the MD simulation on HIV-1 PR.

of structural stability in the simulation; plots of this quantity for the MD on the native and mutant forms are shown in Figure 2c. The rms difference between the MD and the crystal structure in the native protease simulation equilibrated at ~1.3 Å from the starting structure and showed stable behavior for the duration of

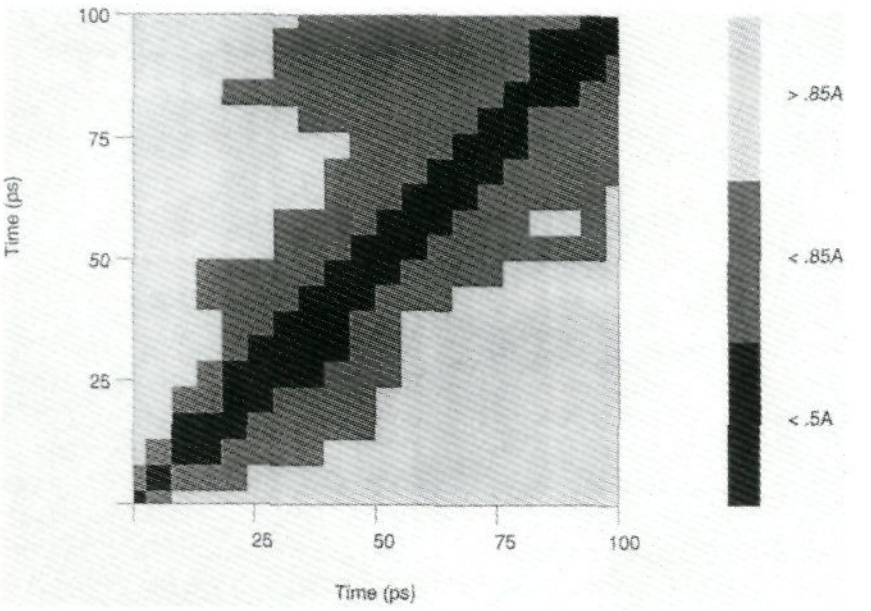

Figure 3. Calculated evolution of the root mean square plot for 5-ps time block averaged structures from the wild-type (upper triangle) and Gln88 mutant (lower triangle).

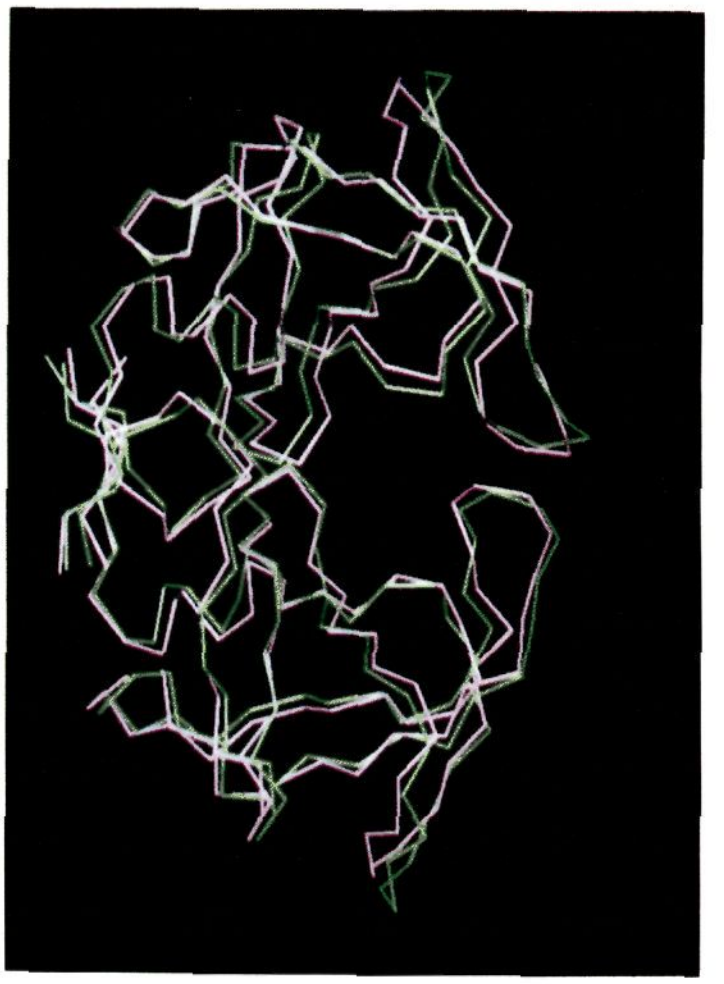

Figure 4. Superposition of the average structures obtained from MD simulation of the wild-type (magenta) and Gln88 mutant (green) protease.

the simulation. A plot of rms deviation from the starting structure in the simulation of the mutant form deviates significantly more from the crystal form than the native MD and was still drifting upward when the simulation was terminated; the rms deviation from the crystal form at this point was ~1.8 Å.

A more detailed view of the evolution of rms deviation of the mutant MD structure as compared with those of the native obtained previously[7,9] is shown in Figure 3. Here the 5-ps block average structures in the simulation are calculated, and the rms deviation of each structure with respect to all the others is calculated, collected in matrix form in order of appearance in the trajectory, and contoured in Figure 3. Utilizing half of the total rms deviation, i.e., <0.85 Å, as a criterion for similarity, plateaus in Figure 3 indicate regions of related structures. The simulation of the native protease (upper triangle) reaches structural equilibration at 40 ps, with the final plateau encompassing the final 60 ps of the simulation.

The corresponding results for the mutant form are shown in the lower triangle of Figure 3. A sequence of transient inter-

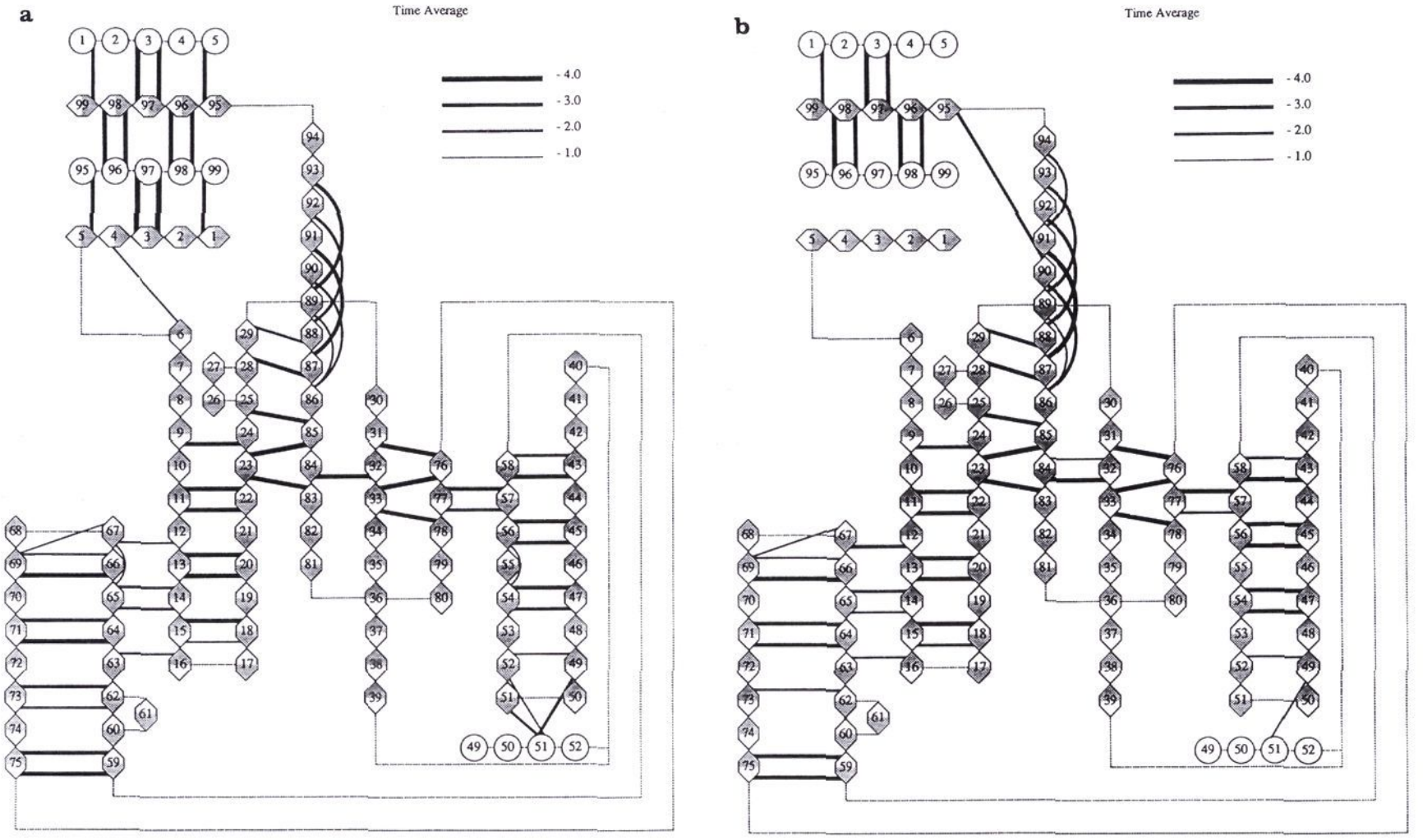

Figure 5. Topology of the secondary structure and the calculated hydrogen-bonding pattern for the backbone of native (left) and Gln88 mutant (right) HIV-1 protease. Solid lines indicate the hydrogen bonds and their relative strength; broken lines indicate the backbone peptide bonds, with the residues in hexagons; residue numbers in circles are for the other chain in the dimer.

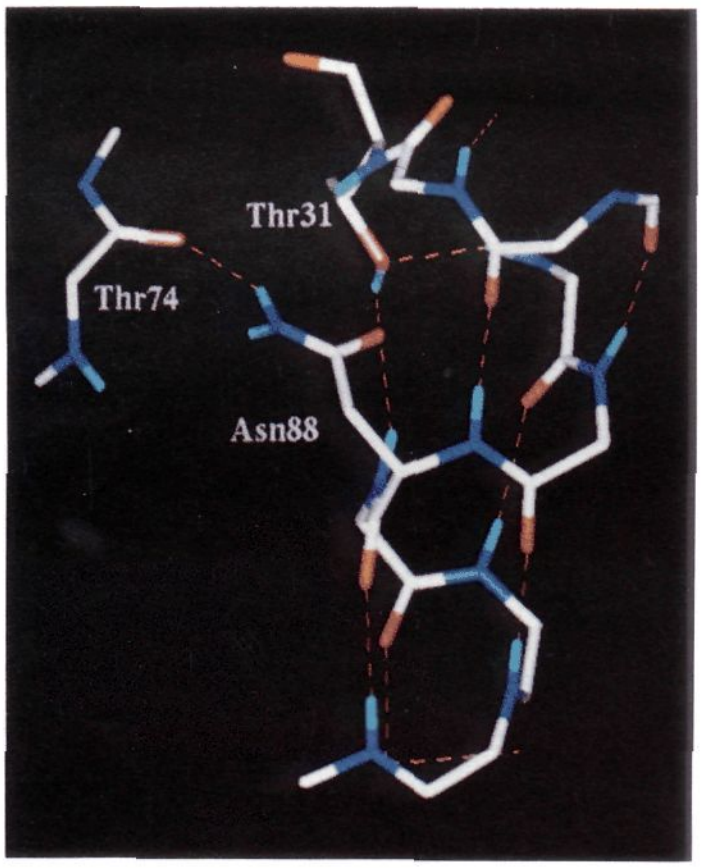

Figure 6. Local hydrogen-bond environment around residue Asn88 obtained previously from MD simulation on the wild-type enzyme.

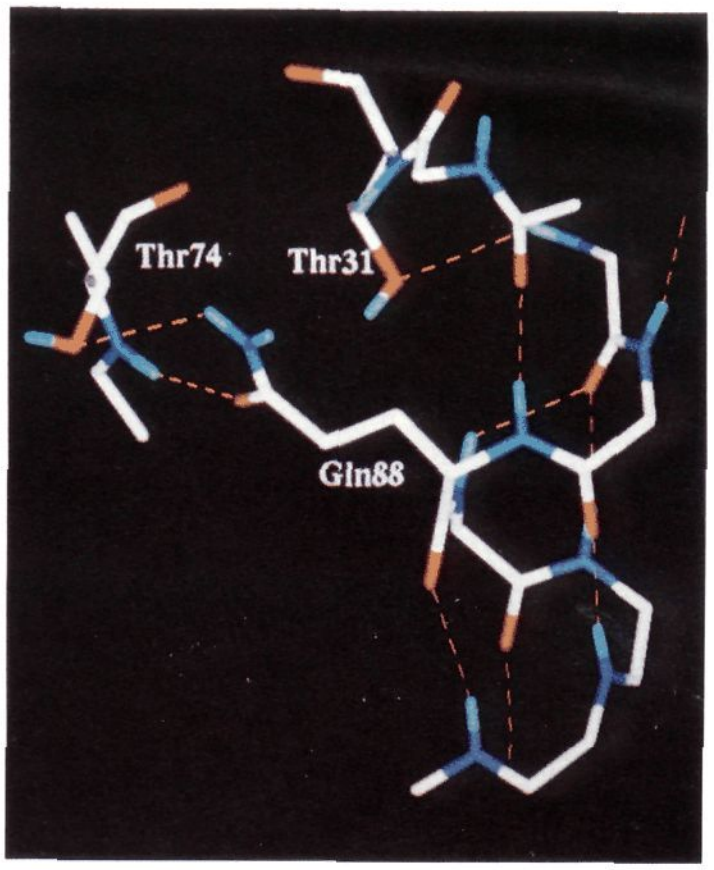

Figure 7. Local hydrogen-bond environment around residue Gln88 obtained from MD simulation on the mutant enzyme.

mediate structures is indicated along the diagonal, none of which persists for more than 30 ps of simulation time. This indicates that the simulation of the mutant form has not yet achieved structural equilibration.

The introduction of the Gln88 mutant introduces some significant changes in the tertiary structure to the enzyme. A superposition of the average structures from the MD simulations on the native and mutant forms is shown in Figure 4. The deviation is significant in the active site (residues 25–27), the flap region (42–58), and the dimer interface (1–5, 95–99). The majority of the residues in the active site and flap region differ by more than 1 Å, and some changes as large as 2.5 Å are observed. The dimer interface is particularly different, with deviations as large as 4.3 Å. The calculated temperature factors of the mutant (not shown) are, in general, higher than those of the native enzyme simulation, consistent with the lack of structural equilibration observed during the course of the simulation.

Analysis of the simulation has established that the MD of the mutant form is destabilized with respect to that of the native. The calculated hydrogen-bond topology of the native and the Gln88 mutant HIV-1 PR are shown in Figures 5a and b, respectively. The backbone hydrogen bonds are indicated as solid lines, with

a thickness proportional to the calculated average bond strength. The majority of the secondary structure retains its antiparallel β-sheet character, but there are some significant changes in the dovetailed, β-pleated sheet at the dimer interface. Most notably, one strand of the dimer interface (1–5 of one monomer) is completely dissociated from its β-strand partner, and other hydrogen bonds in this region are altered. Fully half of the backbone hydrogen-bonding interactions between the monomers, both in the interface and flap region, are absent. Some additional structural changes are observed in the flap region (42–58) of the mutant as well. Two of the flap–flap hydrogen bonds between monomeric proteases predicted in the MD of the native form are absent in the simulation on the mutant. The helix (86–94), containing residue 88, appears to extend to residue 95, altering its participation in the dimer interface. Thus the overall destabilization observed in the simulation on the mutant form is linked to incipient dissociation of the dimer.

A consideration of the local environment about residue 88 provides details on the mechanism of the destabilization. The previous MD simulation showed that the amide side chain of Asn88 in the native protease is involved in three hydrogen bonds (Figure 6). The amide carbonyl is hydrogen bonding with the hydroxyl side chain of Thr31 as well as with a backbone amide hydrogen from residue 89. The amide nitrogen of Asn88 is a hydrogen-bond donor with the backbone of residue 74. In the mutant Gln88 form, the amide side chain is shifted due to the introduction of a methylene group, placing a hydrogen-bond acceptor where a donor was previously located (Figure 7). The local hydrogen-bond framework is changed to accommodate this perturbation, with the Gln side chain now bonded to the side-chain hydroxyl oxygen and amide hydrogen from Thr74 as the only interactions. This results in a net change of one hydrogen bond within one monomer.

In summary, the calculations predict the following mechanism for the destabilization of the Gln88 mutant of the HIV-1 PR dimer: the introduction of Gln at residue 88 results in a net loss of one hydrogen bond locally in the structure. The corresponding structural reorganization causes a loss of articulation in backbone hydrogen bonding at the dimer interface, destabilizing the dimeric structure. It is important to note that the simulation did not achieve structural equilibration within 100 ps. It is therefore not possible to address whether the mutant dimer might adopt a stable conformation, given longer simulation times. However, the observed destabilization in the dimer interface provides leading evidence for dimer dissociation. These results provide a plausible mechanistic explanation for the destabilization of dimeric protease mutated at residue 88 and contribute to a general understanding of the nature of protein–protein interactions at the molecular level.

Acknowledgment. This research was supported by Grant No. GM 37909 from the National Institutes of Health and a Cooperative High Technology Research and Development from the State of Connecticut to Wesleyan University and Bristol-Myers Squibb. Computer facilities were provided by the Pittsburgh Supercomputer Center. Discussions with Dr. S. Swaminathan are gratefully acknowledged.